

Kinetic Studies of the Reactions of Atomic Hydrogen with Iodoalkanes

Jessie Yuan,[†] Leah Wells,[†] and Paul Marshall^{*,†,‡}

Department of Chemistry, University of North Texas, PO Box 5068, Denton, Texas 76203,
and Center for Computational Modeling of Nonstructural Materials, Wright Laboratory,
Wright–Patterson Air Force Base, Ohio 45433

Received: December 16, 1996; In Final Form: February 26, 1997[⊗]

Rate constants for the reaction of H atoms with the alkyl iodides iodomethane (**1**), deuterated iodomethane (**1d**), iodoethane (**2**), 2-iodopropane (**3**), and 2-iodo-2-methyl propane (**4**) have been measured using the flash-photolysis resonance fluorescence technique. The results are $k_1 = (6.3 \pm 0.6) \times 10^{-11} \exp[(-5.0 \pm 0.3) \text{ kJ mol}^{-1}/RT]$ ($T = 297\text{--}757 \text{ K}$), $k_{1d} = (8.0 \pm 1.7) \times 10^{-11} \exp[(-5.3 \pm 0.7) \text{ kJ mol}^{-1}/RT]$ ($T = 296\text{--}728 \text{ K}$), $k_2 = (1.1 \pm 0.2) \times 10^{-10} \exp[(-5.9 \pm 0.8) \text{ kJ mol}^{-1}/RT]$ ($T = 295\text{--}624 \text{ K}$), $k_3 = 1.4 \times 10^{-11}$ ($T = 295 \text{ K}$) and $k_4 = 2.0 \times 10^{-11}$ ($T = 294 \text{ K}$) $\text{cm}^3 \text{ molecule}^{-1} \text{ s}^{-1}$. The transition state for the substitution reaction $\text{H} + \text{CH}_3\text{I} \rightarrow \text{I} + \text{CH}_4$ was characterized at the Gaussian-2 level of ab initio theory, and the process was shown to be slow. Evidence is presented showing that H-atom abstraction is also slow, and that the dominant pathway for the reactions of H atoms with iodoalkanes is I-atom abstraction.

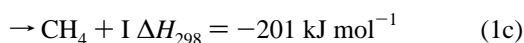
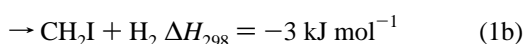
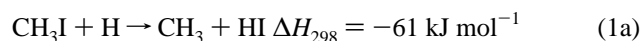
Introduction

There is growing interest in the combustion chemistry of iodine compounds, arising from the search for substitutes for the halon fire-extinguishing agents CF_3Br and CF_2ClBr .¹ Halon production is banned under the Montreal Protocols on Substances that Deplete the Ozone Layer. CF_3I is a potential candidate for service as a new fire suppressant, but there is a lack of kinetic information on the reactions of iodine-containing compounds, especially at elevated temperatures. Modeling of the radical inhibition chemistry of CF_3I suggests that significant destruction of H-atom chain carriers occurs via the reaction



following the formation of CH_3I in flames by $\text{CH}_3 + \text{I}$ recombination.² It has been argued that reaction 1 is the dominant pathway for CH_3I consumption in a stoichiometric CH_4/air flame.³

To date there have been several studies of reaction 1 at room temperature,^{4,5,6,7} but the temperature dependence of the rate constant k_1 has not been measured. On the basis of the thermochemistry of CH_2I^8 and other species,⁹ there are three exothermic product channels have been determined:



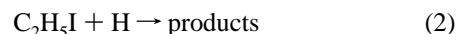
The transition state for 1a has been characterized computationally by Schiesser et al.¹⁰ Marshall et al.³ have analyzed the transition states for channels 1a and 1b using the Gaussian-2 methodology of Pople and co-workers,¹¹ as extended to iodine compounds by Glukhovtsev et al.,¹² and derived high-temperature ab initio rate constants and branching ratios for H vs I abstraction. This analysis is extended in the present work to the displacement channel 1c. The temperature-dependent rate

constant for

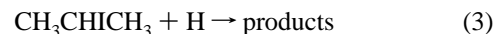


has also been measured, in order to assess the kinetic isotope effect.

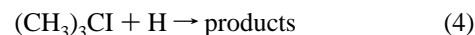
There has been a single study¹³ of



which yielded an experimental room temperature value of k_2 about 2 orders of magnitude smaller than literature values for k_1 . The present work describes the first measurements of the temperature dependences of k_1 and k_2 , and resolves the discrepancy. There is one prior determination¹³ of the rate constant for



while



appears not to have been studied previously. In this work, reactions 3 and 4 have been measured at room temperature. Structural factors that contribute to the reactivity of iodoalkanes are considered, and the reactivities of primary, secondary, and tertiary C–I bonds are compared. Likely products are discussed, and the results are compared with ab initio information about channels 1a–c.

Experimental Method

The experimental apparatus and modifications for H-atom kinetics have been described elsewhere.^{14,15,16} Briefly, atomic H was generated by pulsed flash lamp photolysis of NH_3 , through MgF_2 optics, in the presence of a large excess of iodoalkane. The nominal discharge time was 7 μs . All experiments were carried in Ar bath gas at a total pressure P , and the reagent concentrations were derived from P and the mole fractions of reagents in mixtures made in darkened glass bulbs. The relative concentration of H was monitored using time-resolved resonance fluorescence at a wavelength of 121.6 nm. Fluorescence was detected with a solar-blind photomul-

[†] Department of Chemistry.

[‡] Center for Computational Modeling of Nonstructural Materials.

[⊗] Abstract published in *Advance ACS Abstracts*, April 15, 1997.

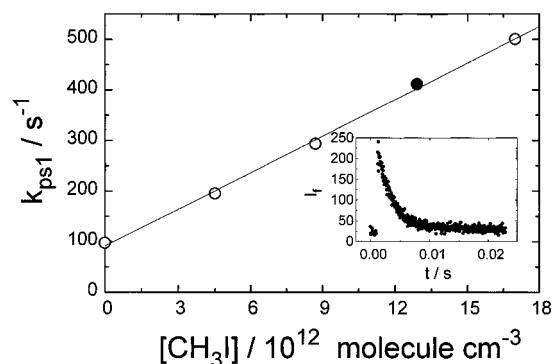


Figure 1. Plot of pseudo-first-order rate constant k_{ps1} vs $[CH_3I]$ at $P = 70$ mbar and $T = 512$ K. The inset shows the time-resolved fluorescence intensity I_f for the filled point.

tiplur tube employed with pulse counting and signal averaging. Under pseudo-first-order conditions and fixed $[NH_3]$,

$$d[H]/dt = -(k_X[X] + k_{diff})[H] = -k_{ps1}[H] \quad (5)$$

where X is an iodoalkane and k_{diff} accounts for loss of H atoms out of the reaction zone other than by reaction with X. k_{diff} increased as the pressure was lowered, and increased modestly as the temperature was raised, which is consistent with the idea that k_{diff} reflected mainly diffusion of H atoms to the reactor walls. k_{ps1} was obtained by fitting the observed fluorescence intensity I_f vs time profiles to an exponential decay (an example is shown as the inset on Figure 1) over typically about four to eight lifetimes. The second-order H + X rate constant k_X was found from linear plots of k_{ps1} vs typically five values of $[X]$, from 0 to $[X]_{max}$ (see Figure 1). This analysis is based on $[X] \gg [H]$. Absolute $[H]$ was not measured (and is not required for the determination of k_{ps1}), and a verification that pseudo-first-order conditions were maintained is that the derived k_X values were independent of the initial $[H]$ (see below). This quantity was altered by changing the concentration of NH_3 and/or the photolysis pulse energy. The temperature T in the reaction zone was monitored with a thermocouple, corrected for radiation errors of up to 10 K, before and after each set of k_X measurements, and is expected to be accurate to within $\pm 2\%$.¹⁷ The average residence time of gas mixtures in the heated reactor before photolysis τ_{res} was varied to check for possible pyrolysis of the iodoalkanes, while the energy discharged through the flash lamp F was varied to alter the initial radical concentrations.

The Ar (Air Products, 99.997%) was used directly from the cylinder and NH_3 (MG Industries, 99.99%) was purified by freeze-pump-thaw cycles from 77 K. The iodoalkanes (CH_3I , Aldrich, 99% and 99.5%; CD_3I , Aldrich, 99.5+ atom % D; C_2H_5I , Lancaster, 99%; CH_3CHICH_3 , Aldrich, 99%; $(CH_3)_3CI$, Aldrich, 95%) were purified by distillation to remove any iodine contamination. The C_1 and C_2 reagents were distilled from 273 to 77 K, and the C_3 and C_4 reagents from room temperature to 77 K.

Results

The experimental conditions and results for k_1 , k_{1d} , k_2 , k_3 , and k_4 are summarized in Tables 1–4. The k_1 results were independent of the two different samples of CH_3I employed. The lack of dependence of k_X on F shows that secondary chemistry involving photolysis or reaction products was negligible and that pseudo-first-order conditions were attained, and the lack of dependence of k_1 and k_2 on τ_{res} shows that pyrolysis of CH_3I and C_2H_5I was unimportant at the listed temperatures.

TABLE 1: Rate Constant Measurements for H + CH_3I

T , K	P , mbar	τ_{res} , s	F , J	$[NH_3]$, 10^{15} molecule cm^{-3}	$[CH_3I]_{max}$, 10^{13} molecule cm^{-3}	$k_1 \pm \sigma_{k_1}$, 10^{-11} cm^3 molecule $^{-1}$ s $^{-1}$
295	82.2	1.7	4.05	3.35	8.35	0.83 ± 0.02
295	47.5	1.0	4.05	1.93	6.08	0.89 ± 0.02
295	47.5	1.0	6.05	1.93	4.59	0.86 ± 0.01
295						0.86 ± 0.01^a
297	101.3	2.1	4.05	1.87	5.39	0.76 ± 0.02
297	69.0	1.4	6.05	1.47	3.67	0.77 ± 0.02
297	69.0	1.4	1.80	1.47	3.67	0.77 ± 0.02
297	53.0	1.1	4.05	0.82	3.58	0.73 ± 0.05
297						0.76 ± 0.01^a
362	130.5	2.2	4.05	1.19	4.56	1.29 ± 0.03
362	86.7	1.6	6.05	1.08	3.99	1.22 ± 0.06
362	86.7	1.6	1.80	1.08	3.99	1.21 ± 0.07
362	70.1	0.8	4.05	0.72	2.73	1.00 ± 0.03
362						1.16 ± 0.08^a
427	83.6	1.2	4.05	0.89	1.43	1.42 ± 0.06
427	132.0	1.9	6.05	1.40	3.32	1.60 ± 0.03
427	132.0	1.9	1.80	1.40	3.32	1.59 ± 0.04
427	68.5	0.7	4.05	0.62	1.54	1.38 ± 0.02
427						1.45 ± 0.08^a
512	70.7	1.2	4.05	1.28	2.42	2.06 ± 0.11
512	110.6	1.9	4.05	1.73	2.57	1.95 ± 0.05
512	52.1	0.6	4.05	0.82	1.59	1.85 ± 0.11
512	50.5	0.9	4.05	0.99	2.43	1.97 ± 0.08
512						1.96 ± 0.03^a
621	87.2	1.0	4.05	1.13	1.50	2.13 ± 0.09
621	160.8	1.9	4.05	1.41	1.70	2.34 ± 0.05
621	59.4	0.6	4.05	0.67	1.07	2.21 ± 0.10
621	108.6	1.8	4.05	1.13	2.05	2.27 ± 0.09
621						2.28 ± 0.05^a
757	111.1	1.3	4.05	1.26	1.66	3.00 ± 0.07
757	60.0	0.5	4.05	0.71	0.88	2.61 ± 0.15
757	164.3	1.3	4.05	1.47	1.66	2.86 ± 0.08
757	75.6	0.9	4.05	0.83	1.13	2.63 ± 0.20
757						2.89 ± 0.08^a

^a Average value.

TABLE 2: Rate Constant Measurements for H + CD_3I

T , K	F , J	τ , s	P , mbar	$[NH_3]$, 10^{15} cm^{-3} molecule	$[CD_3I]_{max}$, 10^{12} cm^{-3} molecule	$k_{1d} \pm \sigma_{k_{1d}}$, 10^{11} cm^3 molecule $^{-1}$ s $^{-1}$
296	4.05	1.8	89.8	4.53	53.3	1.00 ± 0.04
296	6.05	3.5	117.2	5.78	54.1	0.95 ± 0.07
296	2.45	3.5	117.2	5.78	54.1	0.91 ± 0.08
296	4.05	1.3	62.4	2.77	25.4	1.09 ± 0.06
						1.00 ± 0.03^a
391	4.05	1.4	87.6	1.24	19.9	1.34 ± 0.05
391	6.05	0.9	58.7	1.34	15.6	1.43 ± 0.03
391	2.45	0.9	58.7	1.34	15.6	1.36 ± 0.06
391	4.05	0.7	85.8	0.98	11.6	1.48 ± 0.04
						1.42 ± 0.03^a
516	4.05	1.0	84.9	1.47	8.8	2.33 ± 0.21
516	4.05	0.5	74.6	0.95	7.7	2.35 ± 0.13
516	4.05	1.6	136.6	1.96	9.8	2.58 ± 0.08
						2.50 ± 0.08^a
728	4.05	0.8	90.7	0.60	6.63	3.62 ± 0.14
728	4.05	0.4	91.0	0.35	6.15	3.06 ± 0.24
728	4.05	0.3	66.9	0.27	5.82	3.41 ± 0.20
728	4.05	0.9	70.8	0.69	7.74	3.30 ± 0.13
						3.40 ± 0.11^a

^a Average value.

Data for reactions 1 and 2 at higher temperatures did show consistent variation with τ_{res} , and for reaction 2 showed a decrease in the apparent k_2 above 630 K, and therefore were excluded from further analysis.

The Arrhenius plot for reaction 1 is shown in Figure 2, and the weighted linear fit yields

$$k_1 = (6.3 \pm 0.6) \times 10^{-11} \exp[(-5.0 \pm 0.3) \text{ kJ mol}^{-1} / RT] \text{ cm}^3 \text{ molecule}^{-1} \text{ s}^{-1} \quad (6)$$

The quoted errors in the Arrhenius parameters are 1σ and are

TABLE 3: Rate Constant Measurements for H + C₂H₅I

<i>T</i> , K	<i>P</i> , mbar	τ_{res} , s	<i>F</i> , J	[NH ₃], 10 ¹⁵ molecule cm ⁻³	[C ₂ H ₅ I] _{max} , 10 ¹³ molecule cm ⁻³	$k_2 \pm \sigma_{k_2}$, 10 ⁻¹¹ cm ³ molecule ⁻¹ s ⁻¹
295	76.5	1.6	4.05	1.22	4.62	1.00 ± 0.03
295	55.5	0.9	6.05	0.94	4.18	0.92 ± 0.02
295	55.5	0.9	1.80	0.94	4.18	0.85 ± 0.03
295	109.5	1.7	4.05	0.66	6.62	1.06 ± 0.04
295						0.94 ± 0.04 ^a
357	131.8	2.3	4.05	1.23	3.92	1.42 ± 0.04
357	88.4	1.5	6.05	1.20	5.08	1.59 ± 0.02
357	88.4	1.5	1.80	1.20	5.08	1.50 ± 0.03
357	67.4	0.8	4.05	0.65	3.48	1.36 ± 0.05
357						1.53 ± 0.05 ^a
450	132.8	1.8	4.05	0.86	3.05	1.95 ± 0.05
450	91.3	1.2	6.05	1.49	4.15	2.29 ± 0.03
450	91.3	1.2	1.80	1.49	4.15	2.22 ± 0.03
450	68.0	0.7	4.05	0.83	2.89	2.21 ± 0.08
450						2.21 ± 0.06 ^a
533	129.5	1.8	4.05	0.99	2.71	2.61 ± 0.03
533	85.0	1.0	6.05	0.55	1.99	2.65 ± 0.05
533	85.0	1.0	1.80	0.55	1.99	2.55 ± 0.07
533	69.4	0.6	4.05	0.33	1.79	2.36 ± 0.08
533						2.59 ± 0.04 ^a
624	155.6	2.0	4.05	1.10	3.02	3.95 ± 0.07
624	96.9	0.9	4.05	0.49	1.79	3.75 ± 0.13
624	153.8	1.8	4.05	0.70	2.75	3.88 ± 0.16
624	76.6	0.6	4.05	0.35	1.30	3.58 ± 0.09
624						3.80 ± 0.09 ^a

^a Average value.

statistical only. Consideration of the covariance leads to a 1 σ precision for the fitted k_1 of 3–5%, and allowance for possible systematic errors leads to 95% confidence intervals of $\pm 13\%$. The Arrhenius plot for reaction 1d is also shown in Figure 2, and the weighted linear fit yields

$$k_{1d} = (8.0 \pm 1.7) \times 10^{-11} \exp[(-5.3 \pm 0.7) \text{ kJ mol}^{-1} / RT] \text{ cm}^3 \text{ molecule}^{-1} \text{ s}^{-1} \quad (7)$$

Consideration of the covariance leads to a 1 σ precision for the fitted k_{1d} of 6–10%, and allowance for possible systematic errors leads to 95% confidence intervals of $\pm 19\%$.

The Arrhenius plot for reaction 2 is also shown on Figure 2, and the best fit is

$$k_2 = (1.1 \pm 0.2) \times 10^{-10} \exp[(-5.9 \pm 0.8) \text{ kJ mol}^{-1} / RT] \text{ cm}^3 \text{ molecule}^{-1} \text{ s}^{-1} \quad (8)$$

The 1 σ precision of the fitted k_2 is 5–13%, and allowance for possible systematic errors leads to 95% confidence intervals of $\pm 28\%$ at the extremes of the experimental T range to $\pm 14\%$ at the center. Similar accuracies, about $\pm 20\%$, are expected for reactions 3 and 4 which were studied at room temperature only (see Table 4).

TABLE 4: Rate Constant Measurements for H + CH₃CHICH₃ and (CH₃)₃CI

iodoalkane, X	<i>T</i> , K	<i>P</i> , mbar	τ_{res} , s	<i>F</i> , J	[NH ₃], 10 ¹⁵ molecule cm ⁻³	[X] _{max} , 10 ¹³ molecule cm ⁻³	$k_X \pm \sigma_{k_X}$, 10 ⁻¹¹ cm ³ molecule ⁻¹ s ⁻¹
CH ₃ CHICH ₃	295	129.0	2.0	4.05	1.19	4.87	1.49 ± 0.02
	295	77.5	1.2	1.80	0.71	3.64	1.39 ± 0.02
	295	77.5	1.2	6.05	0.71	3.64	1.42 ± 0.03
	295	66.0	0.8	4.05	0.44	2.70	1.48 ± 0.04
	295						1.44 ± 0.03 ^a
(CH ₃) ₃ CI	294	129.6	2.7	4.05	1.47	4.34	1.88 ± 0.05
	294	84.3	1.3	6.05	1.04	3.11	2.05 ± 0.04
	294	84.3	1.3	1.80	1.04	3.11	2.00 ± 0.04
	294	68.9	0.7	4.05	0.53	2.10	1.95 ± 0.07
	294						1.99 ± 0.04 ^a

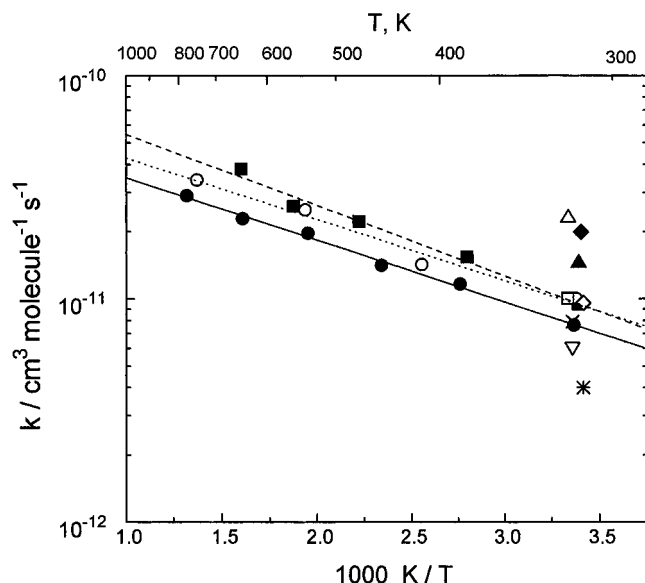
^a Average value.

Figure 2. Arrhenius plot of rate constants for H reactions with CH₃I (● and solid line, this work; X ref 4; ◇, ref 5; ▽, ref 6; *, ref 7), CD₃I (○ and dotted line, this work), C₂H₅I (■ and dashed line, this work; □, ref 13 corrected), C₃H₇I (▲, this work; △, ref 13 corrected) and C₄H₉I (◆, this work).

Discussion

Our k_1 values are compared with four previous measurements in Figure 2 and Table 5, and it may be seen that there is particularly good accord with the most recent literature value, which was obtained by a similar technique.⁷ There is a single previous determination of k_2 , based on a rate measurement relative to



and which Rebbert et al. reported as $k_2 = 7 \times 10^{-14} \text{ cm}^3 \text{ molecule}^{-1} \text{ s}^{-1}$.¹³ This is a factor of 150 smaller than measured here, because Rebbert et al. apparently used an incorrect value of $k_9 = 1.7 \times 10^{-13} \text{ cm}^3 \text{ molecule}^{-1} \text{ s}^{-1}$.¹³ At room temperature $k_9 \approx 2.4 \times 10^{-11} \text{ cm}^3 \text{ molecule}^{-1} \text{ s}^{-1}$.^{18,19,20} Using the same k_2/k_9 as Rebbert et al., the corrected k_2 is then $1.0 \times 10^{-11} \text{ cm}^3 \text{ molecule}^{-1} \text{ s}^{-1}$, close to the present value. The same explanation accounts for much of the discrepancy between the value of k_3 given by Rebbert et al.,¹³ $1.6 \times 10^{-13} \text{ cm}^3 \text{ molecule}^{-1} \text{ s}^{-1}$, and our own direct measurement (Table 5) which is 90 times higher. The corrected k_3 is $2.3 \times 10^{-11} \text{ cm}^3 \text{ molecule}^{-1} \text{ s}^{-1}$ which is in good accord with our result. There appear to be no literature values for k_4 .

As noted in the introduction, three possible reaction pathways for the H plus iodoalkane reactions are I-abstraction, H-abstraction, and I-substitution. These are all bimolecular processes, consistent with the observed pressure independence

TABLE 5: Summary of H + Iodoalkane Measurements

reaction	method	room temperature k , $10^{-11} \text{ cm}^3 \text{ molecule}^{-1} \text{ s}^{-1}$	A , 10^{-11} cm^3 $\text{molecule}^{-1} \text{ s}^{-1}$	E_a , kJ mol^{-1}	lit.
H + CH ₃ I	discharge flow—mass spectrometry	0.4 ± 0.1			ref 4
	flash photolysis—UV absorption	0.96 ± 0.05			ref 5
	pulsed radiolysis—IR absorption	0.61 ± 0.05			ref 6
	flash photolysis—resonance fluorescence	0.79 ± 0.08			ref 7
	flash photolysis—resonance fluorescence	0.83 ± 0.11	6.3 ± 0.6	5.0 ± 0.3	this work
H + CD ₃ I	flash photolysis—resonance fluorescence	0.94 ± 0.18	8.0 ± 1.7	5.3 ± 0.7	this work
H + C ₂ H ₅ I	steady photolysis—relative to H + HI	1 ^a (0.007 ^b)			ref 13
	flash photolysis—resonance fluorescence	1.0 ± 0.3	1.1 ± 0.2	5.9 ± 0.8	this work
H + CH ₃ CHICH ₃	steady photolysis—relative to H + HI	2.3 ^a (0.016 ^b)			ref 13
H + (CH ₃) ₃ CI	flash photolysis—resonance fluorescence	1.4 ± 0.3			this work
	flash photolysis—resonance fluorescence	2.0 ± 0.4			this work

^a Corrected (see text). ^b Uncorrected literature value.

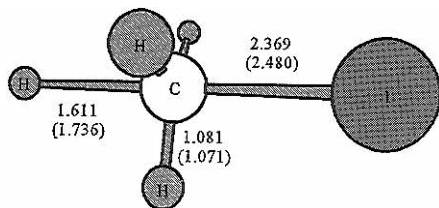


Figure 3. Ab initio geometries of the C_{3v} transition state for $\text{H} + \text{CH}_3\text{I} \rightarrow \text{CH}_4 + \text{I}$. MP2=full/6-31G(d) data shown (HF/6-31G(d) in parentheses). Distances are in 10^{-10} m and the ICH angles are 96.6° (95.8°).

TABLE 6: Ab Initio Results for the Transition State for H + CH₃I → CH₄ + I

HF/6-31G(d) frequencies ^a	1199i, 348, 410 (2), 1082 (2), 1187, 1541 (2), 3313, 3495 (2)
MP2=full/6-31G(d) frequencies ^a	1674i, 463, 470 (2), 1160 (2), 1255, 1464 (2), 3193, 3375 (2)
MP2/6-311G(d,p) ^b	-6957.17377
MP4/6-311G(d,p) ^b	-6957.21271
QCISD(T)/6-311G(d,p) ^b	-6957.21898
MP2/6-311+G(d,p) ^b	-6957.17498
MP4/6-311+G(d,p) ^b	-6957.21407
MP2/6-311G(2df,p) ^b	-6957.23020
MP4/6-311G(2df,p) ^b	-6957.27893
MP2/6-311+G(3df,2p) ^b	-6957.25902
G2[all-electron] ^b	-6957.31294

^a Unscaled, in cm^{-1} . (2) denotes doubly degenerate modes. ^b G2 energy component, in au; 1 au $\approx 2625 \text{ kJ mol}^{-1}$.

of the rate constants. Searches at up to the QCISD/6-311G(d,p) level of theory showed no evidence of a bound $\text{H} + \text{CH}_3\text{I}$ intermediate, whose formation would likely be pressure dependent. The most exothermic of the bimolecular channels is displacement of the I atom. We have characterized the transition state for this process at the HF/6-31G(d) and MP2=full/6-31G(d) levels of theory, and the geometry is shown in Figure 3. Higher level single-point energy calculations yielded the G2 energy (see Table 6) which approximates a QCISD(T)/6-311+G(3df,2p) result.^{11,12} Computations were carried out with the Gaussian 94 program suite.²¹ Relative to the G2 energy of $\text{H} + \text{CH}_3\text{I}$,¹² the G2 barrier to substitution at 0 K is predicted to be 45 kJ mol^{-1} . The size of this barrier indicates that I-atom displacement is kinetically unfavorable. Furthermore, the transition state for this process is found to be tight. The unscaled MP2=full/6-31G(d) frequencies (Table 6) and the geometry, together with entropy data for H and CH₃I,²² lead to an entropy of activation for reaction 1c of $\Delta S^\ddagger_{298} = -91 \text{ J K}^{-1} \text{ mol}^{-1}$ and an implied preexponential factor at 298 K of about $2 \times 10^{-13} \text{ cm}^3 \text{ molecule}^{-1} \text{ s}^{-1}$, more than 2 orders of magnitude below that observed. Substitution will therefore make a negligible contribution to the total k_1 .

TABLE 7: Comparison of Iodoalkane Properties at Room Temperature

iodoalkane, X	k (298 K) for H abstraction, ^a $\text{cm}^3 \text{ molecule}^{-1} \text{ s}^{-1}$	measured k_X (298 K), cm^3 $\text{molecule}^{-1} \text{ s}^{-1}$	$\text{DH}_{298}(\text{C}-\text{I})$, ^b kJ mol^{-1}
CH ₃ I	5.6×10^{-19}	8.3×10^{-12}	237.2 ± 1.3
C ₂ H ₅ I	3.8×10^{-17}	1.0×10^{-11}	236.8 ± 1.7
CH ₃ CHICH ₃	5.3×10^{-17}	1.4×10^{-11}	238.4 ± 2.4
(CH ₃) ₃ CI	6.8×10^{-17}	2.0×10^{-11}	230.1 ± 2.8

^a Empirical estimate (see text). ^b Based on the following $\Delta_f H_{298}$ data, in kJ mol^{-1} : from ref 9, (I) 106.8, (CH₃) 145.8 ± 1.0, (CH₃I) 15.4 ± 0.9, (C₂H₅I) -9.0 ± 0.9, (CH₃CHICH₃) -41.6 ± 1.7, and ((CH₃)₃CI) -72.0 ± 2.2; from ref. 25, (C₂H₅) 121.0 ± 1.5, (CH₃CHCH₃) 90.0 ± 1.7, and ((CH₃)₃C) 51.3 ± 1.8.

An approximate idea of the rate constant for channel 1b can be obtained by comparison with the analogous reaction



for which k_{10} is approximately $7.4 \times 10^{-19} \text{ cm}^3 \text{ molecule}^{-1} \text{ s}^{-1}$ at 298 K.²³ This is about 10^{-7} of k_1 at room temperature, and therefore it can be safely assumed that H abstraction plays a negligible role in reaction 1. This is a reasonable comparison, bearing in mind the similar C-H bond strengths in CH₄ and CH₃I of 440 ± 1 and $431 \pm 8 \text{ kJ mol}^{-1}$, respectively.⁸ A similar assessment of H-abstraction can be made for the heavier iodoalkanes. In these molecules all of the C-H bonds are primary, and the rate constant for H-abstraction from iodoalkanes was estimated as $n/6$ times the rate constant for $\text{H} + \text{C}_2\text{H}_6$ ($4.5 \times 10^{-17} \text{ cm}^3 \text{ molecule}^{-1} \text{ s}^{-1}$ at 298 K²³), where n is the number of C-H bonds. The results are shown in Table 7, and in all cases the H-abstraction channel is minor. An earlier ab initio analysis of reaction 1 also showed that H-atom abstraction is slow.³ This conclusion is reinforced by consideration of the measured kinetic isotope effect, k_1/k_{1d} , which as seen from Figure 2 is slightly less than 1. Had C-H(D) bond breaking been the rate-determining step then the expected ratio k_1/k_{1d} at 298 K would have been around 8.²⁴ In summary, k_1 can be identified with k_{1a} .

k_X at 298 K and the C-I bond dissociation enthalpy DH_{298} are compared in Table 7. DH_{298} values were derived from literature enthalpies of formation for alkyl radicals²⁵ and iodoalkanes, methyl radicals and I atoms.⁹ There is a monotonic trend for k_X along the series of CH₃I and primary to tertiary C-I bonds. (CH₃)₃CI has the weakest C-I bond and is the most reactive alkyl iodide, but any correlation with DH_{298} is unclear. If the variation of k_1 to k_4 were due entirely to activation energy differences, a decrease of only 2.4 kJ mol^{-1} would account for the variation. This change is comparable to the experimental uncertainty in DH_{298} .

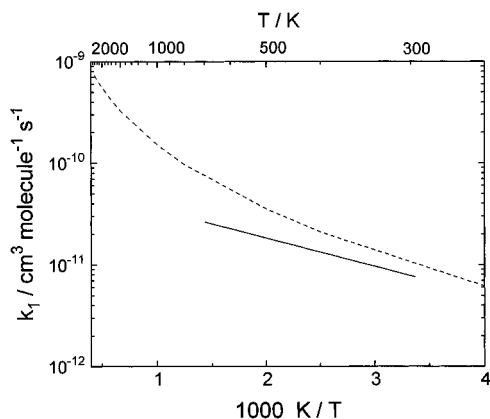


Figure 4. Comparison of measured k_1 for $\text{H} + \text{CH}_3\text{I}$ (solid line, this work) with ab initio results (dashed line, ref 3).

Finally, we note that there is reasonable accord between the earlier ab initio prediction³ for k_1 and the present measurements: at 298 K the ab initio rate constant is higher than our experimental value by a factor of 1.15, increasing to a factor of 2.9 at 760 K. As seen in Figure 4, the discrepancies at higher temperatures arise from the higher curvature predicted for the Arrhenius plot of k_1 . A possible explanation for this behavior is that variational effects are important in this system, and therefore that conventional transition state theory analysis overestimates k_1 .²⁶ Such effects are generally more likely to be significant for reactions with smaller energy barriers, as is the case here.

Conclusions

The temperature dependences of the rate constants for reactions of H atoms with CH_3I , CD_3I , and $\text{C}_2\text{H}_5\text{I}$ have been measured for the first time, and room temperature rate constants for $\text{H} + \text{CH}_3\text{CHICH}_3$ and $\text{H} + (\text{CH}_3)_3\text{CI}$ have also been determined. The results are consistent with I-abstraction as the main reaction pathway, and any contributions from I-substitution and H-abstraction are small.

Acknowledgment. We thank the Robert A. Welch Foundation (Grant B-1174), the Air Force Office of Scientific Research, and the UNT Faculty Research Fund for financial support and the anonymous referees for valuable comments. Computer time was provided by the Wright Laboratory, Wright-Patterson AFB.

References and Notes

(1) Tsang, W.; Miziolek, A. W., Eds. *Halon Replacements: Technology and Science*; ACS Symposium Series 611; Washington, DC, 1995.

- (2) Noto, T.; Babushok, V.; Burgess, D. R., Jr.; Hamins, A.; Tsang, W.; Miziolek, A. 26th International Symposium on Combustion.
- (3) Marshall, P.; Misra, A.; Berry, R. *J. Chem. Phys. Lett.* **1997**, 265, 48.
- (4) Leipunskii, I. O.; Morozov, I. I.; Tal'roze, V. L. *Dokl. Phys. Chem.* **1971**, 198, 547. Russ. orig. p. 136.
- (5) Levy, M. R.; Simons, J. P. *J. Chem. Soc., Faraday Trans. 2* **1975**, 71, 561.
- (6) Sillesen, A.; Ratajczak, E.; Pagsberg, P. *Chem. Phys. Lett.* **1993**, 201, 171.
- (7) Gilles, M. K.; Turnipseed, A. A.; Talukdar, R. K.; Rudich, Y.; Villalta, P. W.; Huey, L. G.; Burkholder, J. B.; Ravishankara, A. R. *J. Phys. Chem.* **1996**, 100, 14005.
- (8) McMillen, D. F.; Golden, D. M. *Ann. Rev. Phys. Chem.* **1982**, 33, 493.
- (9) Lias, S. G.; Bartmess, J. E.; Liebman, J. F.; Holmes, J. L.; Levin, R. D.; Mallard, W. G. *Gas-Phase Ion and Neutral Thermochemistry*; *J. Phys. Chem. Ref. Data* **1988**, 17 (Suppl. 1).
- (10) Schiesser, C. H.; Smart, B. A.; Tran, T.-A. *Tetrahedron* **1995**, 51, 3327.
- (11) Curtiss, L. A.; Raghavachari, K.; Trucks, G. W.; Pople, J. A. *J. Chem. Phys.* **1991**, 94, 7221.
- (12) Glukhovtsev, M. N.; Pross, A.; McGrath, M. P.; Radom, L. *J. Chem. Phys.* **1995**, 103, 1878.
- (13) Rebbert, R. E.; Lias, S. G.; Ausloos, P. *Int. J. Chem. Kinet.* **1973**, 5, 893.
- (14) Shi, Y.; Marshall, P. *J. Phys. Chem.* **1991**, 95, 1654.
- (15) Ding, L.; Marshall, P. *J. Phys. Chem.* **1992**, 96, 2197.
- (16) Goumri, A.; Yuan, W.-J.; Ding, L.; Shi, Y.; Marshall, P. *Chem. Phys.* **1993**, 177, 233.
- (17) Ding, L.; Marshall, P. *J. Chem. Soc., Faraday Trans.* **1993**, 89, 419.
- (18) Baulch, D. L.; Duxbury, J.; Grant, S. J.; Montague, D. C. *Evaluated Kinetic Data for High Temperature Reactions* (Vol. 4); *J. Phys. Chem. Ref. Data* **1981**, 10 (Suppl. 1).
- (19) Lorenz, K.; Wagner, H. Gg.; Zellner, R. *Ber. Bunsen-Ges. Phys. Chem.* **1979**, 83, 556.
- (20) Umemoto, H.; Nakagawa, S.; Tsunashima, S.; Sato, S. *J. Chem. Phys.* **1988**, 124, 259.
- (21) Frisch, M. J.; Trucks, G. W.; Schlegel, H. B.; Gill, P. M. W.; Johnson, B. G.; Robb, M. A.; Cheeseman, J. R.; Keith, T.; Petersson, G. A.; Montgomery, J. A.; Raghavachari, K.; Al-Laham, M. A.; Zakrzewski, V. G.; Ortiz, J. V.; Foresman, J. B.; Peng, C. Y.; Ayala, P. Y.; Chen, W.; Wong, M. W.; Andres, J. L.; Replogle, E. S.; Gomperts, R.; Martin, R. L.; Fox, D. J.; Binkley, J. S.; Defrees, D. J.; Baker, J.; Stewart, J. P.; Head-Gordon, M.; Gonzalez, C.; Pople, J. A. GAUSSIAN 94; Gaussian: Pittsburgh, PA, 1995.
- (22) Gurvich, L.; Veyts, I. V., Alcock, C. B., Eds. *Thermodynamic Properties of Individual Substances*; Hemisphere Pub. Corp.: New York, 1991.
- (23) Baulch, D. L.; Cobos, C. J.; Cox, R. A.; Esser, C.; Frank, P.; Just, Th.; Kerr, J. A.; Pilling, M. J.; Troe, J.; Walker, R. W.; Warnatz, J. *Evaluated Kinetic Data for Combustion Modeling*; *J. Phys. Chem. Ref. Data* **1992**, 21, 411.
- (24) Espenson, J. H. *Chemical Kinetics and Reaction Mechanisms*; McGraw-Hill: New York, 1981; p 203.
- (25) Seakins, P. W.; Pilling, M. J.; Niiranen, J. T.; Gutman, D.; Krasnoperov, L. N. *J. Phys. Chem.* **1992**, 96, 9847.
- (26) Truhlar, D. G.; Isaacson, A. D.; Garrett, B. C. In *Theory of Chemical Reaction Dynamics*; Baer, M., Ed.; CRC Press: Boca Raton, FL, 1985; Vol. 4, Chapter 2.